

Hydroxyacetonitrile (HOCH₂CN) as a precursor for formylcyanide (CHO₂CN), ketenimine (CH₂CNH), and cyanogen (NCCN) in astrophysical conditions

G. Danger¹, F. Duvernay¹, P. Theulé¹, F. Borget¹, J.-C. Guillemin², and T. Chiavassa¹

¹ Aix-Marseille Univ, CNRS, PIIM UMR 7345, 13397 Marseille, France
e-mail: gregoire.danger@univ-amu.fr

² Institut des Sciences Chimiques de Rennes, École Nationale Supérieure de Chimie de Rennes, CNRS, UMR 6226, Avenue du Général Leclerc, CS 50837, 35708 Rennes Cedex 7, France

Received 8 June 2012 / Accepted 19 November 2012

ABSTRACT

Context. The reactivity in astrophysical environments can be investigated in the laboratory through experimental simulations, which provide understanding of the formation of specific molecules detected in the solid phase or in the gas phase of these environments. In this context, the most complex molecules are generally suggested to form at the surface of interstellar grains and to be released into the gas phase through thermal or non-thermal desorption, where they can be detected through rotational spectroscopy. Here, we focus our experiments on the photochemistry of hydroxyacetonitrile (HOCH₂CN), whose formation has been shown to compete with aminomethanol (NH₂CH₂OH), a glycine precursor, through the Strecker synthesis.

Aims. We present the first experimental investigation of the ultraviolet (UV) photochemistry of hydroxyacetonitrile (HOCH₂CN) as a pure solid or diluted in water ice.

Methods. We used Fourier transform infrared (FT-IR) spectroscopy to characterize photoproducts of hydroxyacetonitrile (HOCH₂CN) and to determine the different photodegradation pathways of this compound. To improve the photoproduct identifications, irradiations of hydroxyacetonitrile ¹⁴N and ¹⁵N isotopologues were performed, coupled with theoretical calculations.

Results. We demonstrate that the photochemistry of pure hydroxyacetonitrile (HOCH₂CN) ($\sigma_{\text{photo}} = 5.7 \pm 1.0 \times 10^{-20}$ photon s⁻¹ cm²) under the influence of UV photons, or diluted in water ice ($\sigma_{\text{photo}} = 8.6 \pm 1.0 \times 10^{-20}$ photon s⁻¹ cm²), leads to the formation of formylcyanide (CHO₂CN), ketenimine (CH₂CNH), formaldehyde (CH₂O), hydrogen cyanide (HCN), carbon monoxide (CO), and carbon dioxide (CO₂); the presence of water increases its photodegradation rate. Furthermore, because hydroxyacetonitrile is more highly refractory than water, our results suggest that in astrophysical environments, hydroxyacetonitrile can be formed on icy grains from formaldehyde and hydrogen cyanide, and can be subsequently photodegraded in the water ice, or irradiated as a pure solid at the surface of dry grains after water desorption. As some of the hydroxyacetonitrile photochemistry products are detected in protostellar cores (e.g. formylcyanide or ketenimine), this compound maybe considered as one of the possible sources of these molecules at the grain surface in fairly cold regions. These photoproducts can then be released in the gas phase in a warmer region.

Key words. astrochemistry – methods: laboratory – molecular processes – ISM: molecules

1. Introduction

To detect complex molecules in objects of the solar system, one possibility is in situ analysis, such as the Rosetta mission (Biele & Ulamec 2008; Gulkis & Alexander 2008), or sample return such as the Stardust mission (Brownlee et al. 2003). These missions provide interesting information about the formation of the organic matter in interplanetary environments. For instance, the Stardust mission sample return led to the first detection of glycine (NH₂CH₂COOH) in exogenous environments (Elsila et al. 2009). However, to detect molecules outside the solar system, only telescope observations are available. More than 160 molecules have been detected in the gas phase (Herbst & van Dishoeck 2009) of these environments through rotational spectroscopy. Among them, the aminoacetonitrile (NH₂CH₂CN) (Fig. 1), a potential precursor of glycine, has been detected within the Sagittarius B2 star nursery (Belloche et al. 2008). The detection of molecules inside the solid phase is obtained in the infrared range. The most abundant molecules detected on icy grains are simple, for instance methanol (CH₃OH),

carbon monoxide (CO), carbon dioxide (CO₂), ammonia (NH₃), formaldehyde (CH₂O), or formic acid (HCOOH) (Dartois 2005). The detection of less abundant molecules in interstellar ice from infrared spectra is difficult since they are hidden by strong bands of water and/or silicates (Herbst & van Dishoeck 2009). However, complex molecules formed in the icy grains can be detected indirectly in the gas phase, since they could be sublimated in cold regions through photodesorption (Fayolle et al. 2011; Greenberg 1973), or in warmer regions (Garrod et al. 2008; Noble et al. 2012a). An exchange of molecules always occurs between the gas phase and the solid phase in interstellar environments (Ceccarelli 2008; Garrod et al. 2008). The importance of the grain-surface chemistry is highlighted by the modelling of the gas phase reaction, which underestimates the molecular abundances observed in the gas phase.

Therefore, the formation of complex molecules is mainly suggested to occur at the surface of interstellar grains (Fraser et al. 2002; Herbst & van Dishoeck 2009; Watanabe & Kouchi 2008; de Marcellus et al. 2011; Caro et al. 2002). For instance, this scenario is one of the possibilities to explain the formation

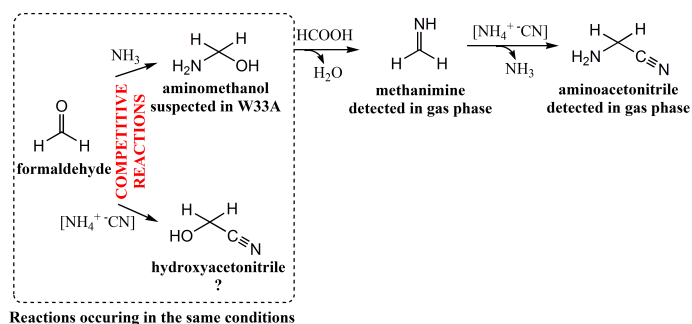


Fig. 1. Experimental pathways in astrophysical conditions for the hydroxyacetonitrile formation via the direct reaction of ammonium cyanide with formaldehyde (ammonium cyanide $[\text{NH}_4^+ \text{CN}^-]$ pathway), and its concurrent reaction, the aminoacetonitrile formation in solid phase via the Strecker synthesis (ammonia (NH_3) pathway).

of $\text{NH}_2\text{CH}_2\text{CN}$ detected in the gas phase. $\text{NH}_2\text{CH}_2\text{CN}$ has indeed been experimentally shown to form in the condensed phase through the photochemistry of acetonitrile and ammonia ice mixture (Danger et al. 2011b), or from the Strecker reaction that occurs at the grain surface (Danger et al. 2011a). However, its relatively low amount compared to the most dominant water molecule does not allow it to be detected on icy grains (Borget et al. 2012). Therefore, it is suggested that the subsequent warming of the grain causes the release of $\text{NH}_2\text{CH}_2\text{CN}$ in the gas phase, which makes it detectable (Belloche et al. 2008; Borget et al. 2012).

Following this scenario, we investigated the possibility of using hydroxyacetonitrile (HOCH_2CN) as a source of interstellar molecules already detected in the gas phase. HOCH_2CN can be formed on the grain surface through the condensation of cyanide (CN^-) and formaldehyde (CH_2O) (Danger et al. 2012). This reaction competes with the first step of the Strecker reaction, which leads to $\text{NH}_2\text{CH}_2\text{CN}$ formation (Fig. 1) (Danger et al. 2012), the first step of which is the aminomethanol formation ($\text{NH}_2\text{CH}_2\text{OH}$). The low-energy barrier difference between these two reactions suggests that if the Strecker scenario is accepted for the formation of a part of the aminoacetonitrile detected in the gas phase, HOCH_2CN has to be considered as an astrophysically relevant compound that could be present in the solid phase in the same environments in which $\text{NH}_2\text{CH}_2\text{OH}$ can be formed and detected (Fig. 1) (Bossa et al. 2009). Following this assumption, we study here the HOCH_2CN photodegradation under VUV irradiation. Our results demonstrate that HOCH_2CN is an interesting precursor of various molecules that are detected in the gas phase of hot cores. Experimental simulations indeed show that through its photodegradation, in dry or water ices, HOCH_2CN could be a precursor of formylcyanide (CHOCN) (Remijan et al. 2008) and ketenimine (CH_2CNH) (Lovas et al. 2006), which are detected in the gas phase of various astrophysical objects. Furthermore, because hydroxyacetonitrile is refractory compared to water, its photochemistry can occur in cold regions where water ices are dominant, or in warmer regions where water has sublimated.

2. Experimental

2.1. Operating systems

Hydroxyacetonitrile, also named glycolonitrile, was synthesized following Gaudry (1955), using KC^{14}N for ^{14}N -hydroxyacetonitrile, or KC^{15}N for ^{15}N -hydroxyacetonitrile. Hydroxyacetonitrile is directly deposited on the cold surface

from its synthesis tube. Therefore, the amount deposited can only be estimated from the infrared spectra. For its irradiation in a water ice, hydroxyacetonitrile is co-deposited with water on the cold surface. Compounds were deposited on a gold-plated surface kept at 40 K with a model 21 CTI cold head. The thickness of the deposited solid films, assuming a density of 0.92 g cm^{-3} for H_2O , is estimated to be around $0.1 \mu\text{m}$, which is consistent with the interstellar ice mantle thickness. The 0.1–1 micron laboratory ices can be considered as optically thin at wavelengths longer than 160 nm (Cottin et al. 2003). However, this is not true for Lyman alpha photons. Therefore, the reported cross sections are upper limits when considering thinner ices, since Lyman alpha does contribute significantly to the measured UV flux used to calculate cross sections.

The warming-up of the samples was performed at a 5 K min^{-1} heating rate using a resistive heater along with a Lakeshore model 331 temperature controller. The infrared spectra of the sample were recorded in a reflection mode between 4000 and 600 cm^{-1} using a Nicolet Magna 750 FTIR spectrometer with an MCT detector. Each spectrum was averaged over one hundred scans with a 1 cm^{-1} resolution. The UV radiations ($\lambda > 120 \text{ nm}$) are generated from a microwave discharge hydrogen flow lamp (Ophos instruments) separated from the vacuum chamber by a magnesium fluoride window. Lamp settings during irradiation are $P_{\text{H}_2} = 300 \times 10^{-3} \text{ mbar}$, microwave forward power 70%, reflected power less than 10%. The distance between the lamp and the ice sample was about 10 cm. The flux was calibrated with the actinometry method described by Cottin et al. (2003) using the photolysis of methanol. The flux of the hydrogen lamp is $1.8 \pm 0.6 \times 10^{15} \text{ photons cm}^{-2} \text{ s}^{-1}$. Uncertainties on kinetic constant and photodissociation cross-sections were estimated from three different experiments with a confidence level of 95% (student value of 4.303 for three experimental values), and they therefore represent the experimental uncertainties.

2.2. Infrared spectroscopy for product attributions and quantifications

To corroborate compound attributions using literature data, vibrational analyses were performed to compute the harmonic vibrational frequencies for the ^{14}N and ^{15}N isotopologues (HOCH_2CN , NCCN , CHOCN , HCN , $\text{NH}=\text{C}=\text{CH}_2$). Nevertheless, to simplify this analysis, we did not take into account the effect of environment on the calculations. Calculations were performed using the Gaussian 98 package (Lee et al. 1988; Frisch et al. 1998) at the B3LYP/6-31G** level, which is known to supply reliable predictions of vibrational wavenumbers (Duvernay et al. 2004, 2007).

We used the band integration strengths to monitor the decrease in the reactant infrared band intensities because they are consumed during the reaction, and to estimate how much of each product is formed. Because of the reflecting mode, the calculated amount of molecules obtained from the band integration was corrected for by a factor 2 since the infrared beam is orthogonal to the sample holder. The amount of formaldehyde was obtained from the band at 1717 cm^{-1} (which has a band strength of $\mathcal{A} = 9.6 \times 10^{-18} \text{ cm molecule}^{-1}$, Schutte et al. 1993), or the band at 1498 cm^{-1} ($\mathcal{A} = 3.9 \times 10^{-18} \text{ cm molecule}^{-1}$, Schutte et al. 1993). The amount of ketenimine $\text{NH}=\text{C}=\text{CH}_2$ was obtained with the band at 2035 cm^{-1} ($\mathcal{A} = 7.2 \times 10^{-17} \text{ cm molecule}^{-1}$, Jacox & Milligan 1963; Hudson & Moore 2004). For the carbon dioxide CO_2 amount, the band at 2340 cm^{-1} was used with a

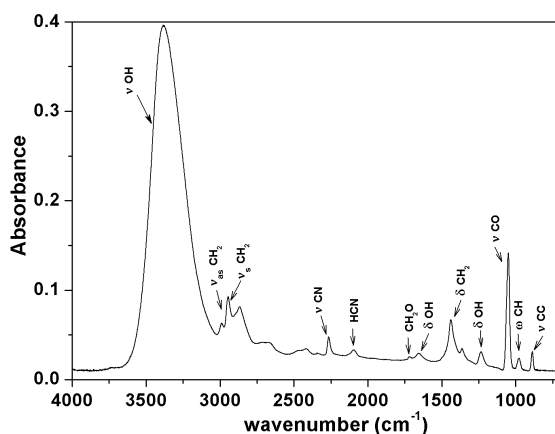


Fig. 2. Pure hydroxyacetonitrile deposited at 40 K directly from its tube synthesis.

band strength of $\mathcal{A} = 7.6 \times 10^{-17}$ cm molecule $^{-1}$ (Gerakines et al. 1995). Since the band strength of the nitrile stretching mode is unknown, for the formyl cyanide CHO-CN, the carbonyl stretching mode of carbonyl was used. Its band strength was approximated to $\mathcal{A} = 1 \times 10^{-17}$ cm molecule $^{-1}$, which is a common value used for carbonyl stretching mode. The amount of carbon monoxide was obtained from the band at 2136 cm $^{-1}$ ($\mathcal{A} = 1.7 \times 10^{-17}$ cm molecule $^{-1}$, Gerakines et al. 1995). For the hydrogen cyanide HCN, the CN stretching mode was used with a band strength of $\mathcal{A} = 5.1 \times 10^{-18}$ cm molecule $^{-1}$ (Hudson & Moore 2004). The nitrile stretching band of acetonitrile grows below the nitrile stretching mode of the hydroxyacetonitrile. The acetonitrile amount was thus obtained by estimating the contribution of hydroxyacetonitrile degradation to the 2265 cm $^{-1}$ band using the hydroxyacetonitrile band at 1050 cm $^{-1}$. The amount of acetonitrile was then estimated by subtracting the amount of photodegraded hydroxyacetonitrile to the band at 2265 cm $^{-1}$.

3. Results and discussion

3.1. Photodegradation of pure hydroxyacetonitrile (HOCH₂CN)

In a previous publication (Danger et al. 2012), we have demonstrated that the hydroxyacetonitrile can be formed in laboratory ice experiments, which simulate the reactions that could occur at the surface of interstellar grains (Fig. 1). In astrophysical environments, molecules can be submitted to several physical processes that could alter them (Throop 2011), such as UV processing. In this section, we are interested in investigating the stability and evolution of the hydroxyacetonitrile under UV irradiation at 40 K. Pure ¹⁴N-hydroxyacetonitrile was deposited directly from its tube synthesis at 40 K. The corresponding infrared spectrum is displayed in Fig. 2, while the experimental band positions for the isotopologues ¹⁴N and ¹⁵N are collected in Table 1, along with their vibrational assignments. We also include in this table the theoretical frequency shifts $\Delta\nu(^{14}\text{N}-^{15}\text{N})$ between the ¹⁴N and the ¹⁵N hydroxyacetonitrile obtained from infra-red spectra and those calculated using the B3LYP/6-31G** level of calculation. The modes that imply nitrogen motion will be the most affected by the isotopic substitution. For example, the stronger calculated frequency shift is obtained for the nitrile mode of 31 cm $^{-1}$, in good agreement with the experimental value of 38 cm $^{-1}$. We use throughout the frequency shift induced by isotopic substitution in the nitrile region to investigate the assignment of the photoproducts.

Table 1. Positions and attributions of infrared absorption bands of pure ¹⁴N and ¹⁵N hydroxyacetonitrile (HOCH₂CN) at 40 K.

Exp ν (cm $^{-1}$)		Identification	$\Delta\nu(^{14}\text{N}-^{15}\text{N})$ (cm $^{-1}$)	
¹⁴ N	¹⁵ N		Exp	Theo
3375	3375	$\nu(\text{O-H})$	0	0
2989	2989	$\nu_{\text{as}}(\text{C-H})$	0	0
2944	2944	$\nu_{\text{s}}(\text{C-H})$	0	0
2265	2227	$\nu(\text{C=N})$	38	31
1655	1655	$\delta(\text{OH})$	0	0
1437	1437	$\delta(\text{CH}_2)$	0	0
1362	1362	$\tau(\text{CH}_2)$	0	0
1233	1241	$\delta(\text{OH})$	-8	0
1050	1053	$\nu(\text{C-O})$	-3	0
977	985	$\omega(\text{CH}_2)$	-8	0
887	882	$\nu(\text{C-C})$	5	0

Notes. The frequency shifts between ¹⁴N and ¹⁵N obtained from experimental or theoretical data are also reported. Vibration mode: stretching (ν), bending (δ), rocking (ρ), torsion (τ), wagging (ω). Type of vibration mode: asymmetric (as), symmetric (s).

After 240 min of irradiation, around 50% of the hydroxyacetonitrile is consumed. The evolution of the absorbance of the band located at 1060 cm $^{-1}$ as a function of the time is fitted by a first-order kinetic rate, giving a kinetic constant of $1.1 \pm 0.2 \times 10^{-4}$ s $^{-1}$. Furthermore, because the photon flux of our lamp is $1.8 \pm 0.6 \times 10^{15}$ photon cm $^{-2}$ s $^{-1}$, the corresponding photodissociation cross-section for the hydroxyacetonitrile is estimated to be $\sigma_{\text{photo}} = 5.7 \pm 1.0 \times 10^{-20}$ photon $^{-1}$ cm 2 . For pure ¹⁵N-hydroxyacetonitrile the kinetic constant is $1.1 \pm 0.2 \times 10^{-4}$ s $^{-1}$, giving a photodissociation cross-section of $\sigma_{\text{photo}} = 5.8 \pm 1.0 \times 10^{-20}$ photon $^{-1}$ cm 2 .

The infrared spectrum obtained after 240 min of VUV irradiation at 40 K shows the appearance of new infrared bands compared to the initial hydroxyacetonitrile (Table 1, and Fig. 2 vs. Fig. 3A). The majority of these new bands appears in the range 2000–2350 cm $^{-1}$. The band at 2341 cm $^{-1}$ is attributed to carbon dioxide (Gerakines et al. 1995), and the one at 2135 cm $^{-1}$ to carbon monoxide (Gerakines et al. 1995). Bands at 2090 cm $^{-1}$, 2168 cm $^{-1}$, and 2235 cm $^{-1}$ are attributed to CN stretching modes of the hydrogen cyanide complex (HCN) (Danger et al. 2011a; Hudson & Moore 2004; Noble et al. 2012b), cyanogen (NCCN) (Hudson & Moore 2004; Stroh et al. 1989), and formylcyanide (CHO-CN) (Lewis-Bevan et al. 1992), respectively. The presence of CHO-CN is strengthened by bands at 1697 cm $^{-1}$, 1370 cm $^{-1}$, and 905 cm $^{-1}$ (Lewis-Bevan et al. 1992). The band at 2035 cm $^{-1}$ is attributed to ketenimine (CH₂CNH) (Hudson & Moore 2004; Jacox & Milligan 1963), which is confirmed by the band at 1125 cm $^{-1}$ (Hudson & Moore 2004; Jacox & Milligan 1963). The two bands at 1720 cm $^{-1}$ and 1498 cm $^{-1}$ are attributed to the formation of formaldehyde (Schutte et al. 1993). Furthermore, the growth of water is also observed with the appearance of bands at 3300 cm $^{-1}$ and 1663 cm $^{-1}$ (Gerakines et al. 1995). The difference spectrum between the deposit and after the 240 min of irradiation shows that new bands also grow under the one of the nitrile stretchings of the hydroxyacetonitrile at 2260 cm $^{-1}$ (Fig. 3B). One band at 2276 cm $^{-1}$ is attributed to the ¹³C carbon dioxide (Gerakines et al. 1995), and another band at 2257 cm $^{-1}$ is tentatively attributed to the nitrile band of acetonitrile (CH₃CN) (d’Hendecourt & Allamandola 1986; Hudson & Moore 2004). Therefore, the photodegradation of hydroxyacetonitrile is

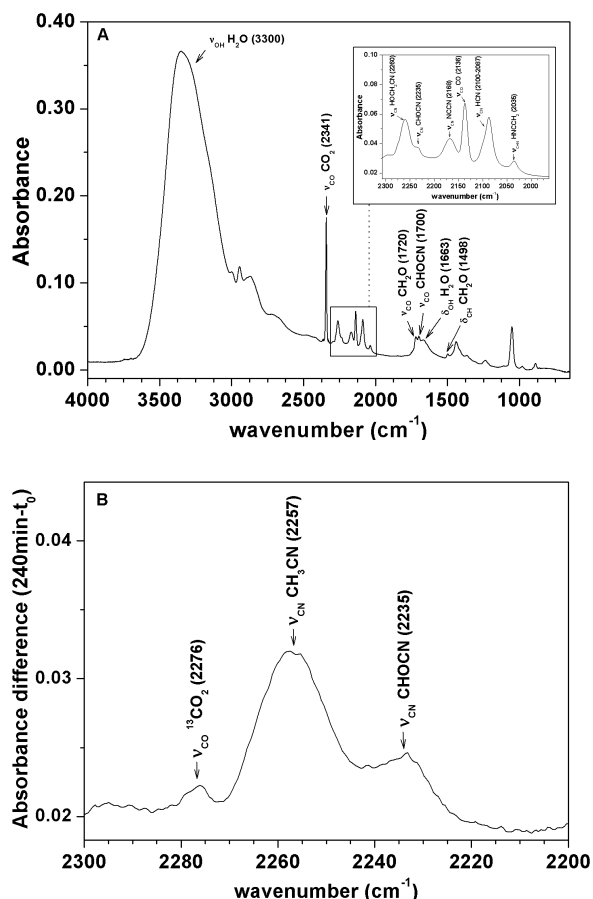


Fig. 3. Infrared spectrum of pure hydroxyacetonitrile after 240 min of VUV irradiations at 40 K **A**), and the difference between spectrum of **A**) with the one of hydroxyacetonitrile before irradiation in the range 2300–2200 cm⁻¹ **B**).

efficient and leads to interesting molecules that are observed in the gas phase of interstellar objects, such as ketenimine (Lovas et al. 2006), formylcyanide (Remijan et al. 2008), formaldehyde, hydrogen cyanide, or acetonitrile (Remijan et al. 2004).

However, photoproduct assignments from infrared spectroscopy in solid state is far from obvious, especially when only one band is observed. Photolysis was performed using the ¹⁵N isotopologue of hydroxyacetonitrile to verify the previous ¹⁴N assignments. We compared the experimental frequency shifts $\Delta\nu$ (¹⁴N-¹⁵N) in the nitrile region (2300–2000 cm⁻¹) with the corresponding theoretical shifts (Table 2), since this region is the most affected by isotopic substitution on nitrogen atoms. We also compared experimental and theoretical frequency shifts in the nitrile region between the reactant ¹⁴N, used as a reference, and the ¹⁴N photoproducts (noted $\Delta\nu$ HOCH₂C¹⁴N in Table 2). Consequently, a photoproduct attribution will be considered as relevant if the following conditions are fulfilled:

- *i* its bands have to be observed from the ¹⁴N isotopologue;
- *ii* its bands have to be observed from the ¹⁵N isotopologue;
- *iii* the experimental and theoretical frequency shifts $\Delta\nu$ (¹⁴N-¹⁵N) in the nitrile region have to be coherent;
- *iv* the observed difference in frequency $\Delta\nu$ HOCH₂C¹⁴N between hydroxyacetonitrile and its daughter products must be consistent with theory.

As shown in Table 2, the comparison between the theoretical and experimental frequency shifts confirms our previous

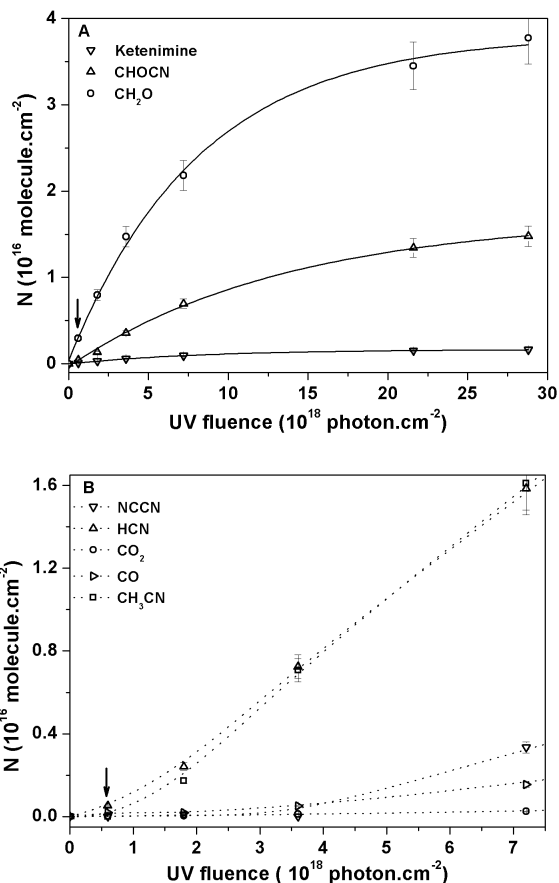


Fig. 4. Evolution of the photo-products from the primary photodegradation pathways of HOCH₂CN at 40 K **A**), and from secondary photodegradation pathways **B**). The arrow refers to the time of the measurement of the photoproducts from the primary photodegradation process of HOCH₂CN.

assignments except for CH₃CN. The calculated frequency shift between HOCH₂CN and CH₃CN is –11 cm⁻¹, while we experimentally observe +8 cm⁻¹. Even if the $\Delta\nu$ (¹⁴N-¹⁵N) is fairly coherent between experimental and theoretical data, these results cannot resolve the ambiguity of the presence of CH₃CN assignment for the observed band at 2257 cm⁻¹ with the ¹⁴N isotopologue (2236 cm⁻¹ for ¹⁵N). The photodegradation of the ¹⁵N isotopologue confirms the CHOCHN, NH=C=CH₂, NCCN, and HCN photoproduct formation, while the CH₃CN attribution remains ambiguous.

After attributing hydroxyacetonitrile photoproducts, we tentatively estimated the different reaction pathways for the hydroxyacetonitrile degradation under VUV irradiation. The bands of products formed during this photochemical process were integrated. By tracing the evolution of the column density as a function of the fluence, it is possible to distinguish the first photodegradation processes from the secondary ones (Fig. 4). The photoformation evolution fittings show a first-order exponential growth with kinetic formation rates of 1.4×10^{-2} s⁻¹ for ketenimine, 8.8×10^{-3} s⁻¹ for formylcyanide, and 1.5×10^{-2} s⁻¹ for formaldehyde (Fig. 4A). These three photoproducts are therefore the first pathways of hydroxyacetonitrile photodegradation (Fig. 5). The branching ratio of the corresponding processes was estimated to be at 5 min of irradiation of 10% for ketenimine, 15% for formylcyanide, and 75% for formaldehyde. Due to the development of secondary photodegradation processes, the branching ratios evolve after 240 min of irradiation,

Table 2. Positions and attributions of infrared absorption bands of photoproducts formed after the VUV irradiation of ^{14}N or ^{15}N hydroxyacetonitrile at 40 K during 240 min.

^a Exp ν (cm^{-1})		Attribution	Identification	^b $\Delta\nu^{14}\text{N}-^{15}\text{N}$ (cm^{-1})		^c $\Delta\nu_{\text{HOCH}_2\text{C}^{14}\text{N}}$ (cm^{-1})		Band strength (cm molecule^{-1})
^{14}N	^{15}N			Exp	Theo	Exp	Theo	
3300	3300	$\nu(\text{O-H})$	H_2O	–	–	–	–	–
2340	2340	$\nu(\text{C=O})$	$^{12}\text{CO}_2$	–	–	–	–	7.6×10^{-17}
2276	2276	$\nu(\text{C=O})$	$^{13}\text{CO}_2$	–	–	–	–	–
2257	2236	$\nu(\text{C}\equiv\text{N})$	CH_3CN	21	30	8	–11	2.2×10^{-18}
2233	2204	$\nu(\text{C}\equiv\text{N})$	CHOCN	29	31	32	19	–
2167	2151	$\nu(\text{C}\equiv\text{N})$	NCCN	16	35	98	109	2.2×10^{-18}
2136	2136	$\nu(\text{C}\equiv\text{O})$	CO	–	–	–	–	1.7×10^{-17}
2087	2054	$\nu(\text{C}\equiv\text{N})$	HCN complex	33	35	178	148	5.1×10^{-18}
2035	2024	$\nu(\text{C=C=N})$	HN=C=CH_2	11	13	230	239	7.2×10^{-17}
1719	1714	$\nu(\text{C=O})$	CH_2O	–	–	–	–	9.6×10^{-18}
1697	1696	$\nu(\text{C=O})$	CHOCN	1	0	568	566	^d 1×10^{-17}
1663	–	$\delta(\text{OH})$	H_2O	–	–	–	–	1.2×10^{-17}
1498	1498	$\nu(\text{C=O})$	CH_2O	–	–	–	–	3.9×10^{-18}
1370	1370	$\delta(\text{CH})$	CHOCN	–	–	–	–	–
1125	1125	$\nu(\text{C-C})$	HN=C=CH_2	–	–	–	–	–
905	–	$\nu(\text{C-C})$	CHOCN	–	–	–	–	–

Notes. The frequency shifts between ^{14}N and ^{15}N ($\Delta\nu^{14}\text{N}-^{15}\text{N}$) obtained from experimental or theoretical data are reported. Experimental and theoretical frequency shifts in the nitrile region between the reactant $\text{HOCH}_2\text{C}^{14}\text{N}$, used as a reference, and the ^{14}N photoproducts are reported ($\Delta\nu_{\text{HOCH}_2\text{C}^{14}\text{N}}$). Band strengths used for the calculation of column densities are also reported. Vibration mode: stretching (ν), bending (δ), rocking (ρ), torsion (τ), wagging (ω). Type of vibration mode: asymmetric (as), symmetric (s). Comb: combination mode. Harmon: harmonic mode. ^(a) These wavenumbers were obtained from the experimental irradiation of hydroxyacetonitrile ^{14}N or ^{15}N . ^(b) These data correspond to the difference between wavenumbers of ^{14}N and ^{15}N species obtained from the experiments (Exp) or from the theoretical calculation (Theo). ^(c) These data were obtained by subtracting the wavenumber of the nitrile stretching mode of the hydroxyacetonitrile to the ones of nitrile stretching mode of photoproducts from experimental (Exp) or theoretical data (Theo). ^(d) The band strength of the hydroxyacetonitrile carbonyl was considered as a general band strength for aldehyde.

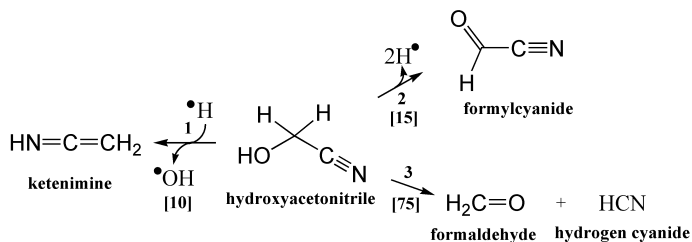


Fig. 5. Primary degradation pathways that occur during the VUV irradiation of pure hydroxyacetonitrile HOCH_2CN . The branching ratios of each pathway are reported in brackets.

giving 35% for ketenimine and acetonitrile, 25% for formylcyanide, and 39% for formaldehyde. Five photoformation evolutions concerning CO_2 , CO , HCN , NCCN , and CH_3CN display a latency period that differs depending on the molecule (Fig. 4B). These formations are therefore considered as secondary photodegradation processes. Figure 6 displays proposed formation pathways of these molecules. The carbon monoxide (CO) could come from the photodegradation of formaldehyde (Eq. (2)), and of formylcyanide (Eq. (1)). The carbon dioxide (CO_2) could be formed by reaction between CO and the hydroxyl radical (OH) (Eq. (4)). The dimerization of CN radical could lead to the cyanogen formation (NCCN , Eq. (3)). Finally, acetonitrile (CH_3CN , Eq. (5)) could be formed by the tautomerization of ketenimine under VUV irradiation.

3.2. Photodegradation of HOCH_2CN in water ice

Water is one of the most abundant molecules that constitutes the icy mantle of interstellar grains in cold regions. In this section, to

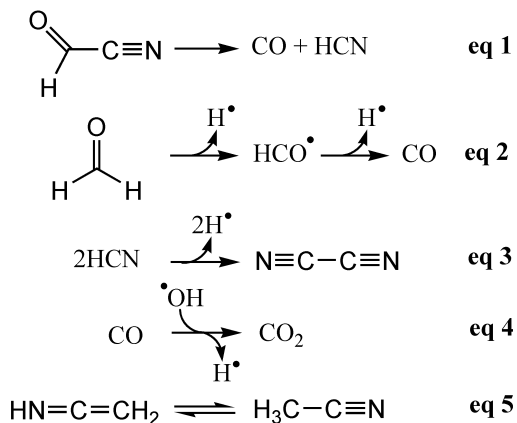


Fig. 6. Propositions for secondary degradation pathways, which occur during the VUV irradiation of pure hydroxyacetonitrile HOCH_2CN .

enhance the astrophysical implication of this work, we describe $\text{HOCH}_2\text{C}^{14}\text{N}$ dilution in water ice (1:10 $\text{HOCH}_2\text{CN}:\text{H}_2\text{O}$). The ratio was estimated from the experimental spectrum by using the band strength of $\text{HOCH}_2\text{C}^{14}\text{N}$ at 1057 cm^{-1} ($\mathcal{A} = 3.1 \times 10^{-17} \text{ cm molecule}^{-1}$, Danger et al. 2012), and the one of water at 3243 cm^{-1} ($\mathcal{A} = 2.0 \times 10^{-16} \text{ cm molecule}^{-1}$, Gerakines et al. 1995). In a water environment, infrared bands present small shifts relative to pure $\text{HOCH}_2\text{C}^{14}\text{N}$, i.e. the band at 2060 cm^{-1} for a pure deposit shifts to 2063 cm^{-1} in a water ice. The evolution under UV irradiation of the absorbance of the band located at 1057 cm^{-1} (1050 cm^{-1} for pure $\text{HOCH}_2\text{C}^{14}\text{N}$) as a function of the time was fitted by a first-order kinetic rate, giving a kinetic constant of $1.7 \pm 0.2 \times 10^{-4} \text{ s}^{-1}$. Furthermore, because the photon flux of our lamp is $1.8 \pm 0.6 \times 10^{15} \text{ photon cm}^{-2} \text{ s}^{-1}$,

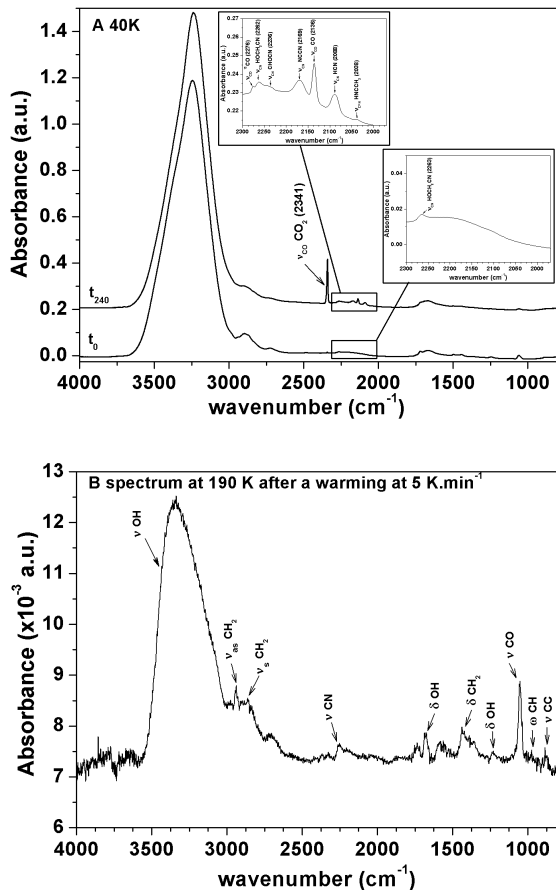


Fig. 7. UV irradiation of HOCH_2CN diluted in a water ice (1:10 $\text{HOCH}_2\text{CN}:\text{H}_2\text{O}$). **A**) Infrared spectra monitored after the $\text{H}_2\text{O}:\text{HOCH}_2\text{CN}$ ice formation at 40 K, t_0 , and after 240 min of VUV irradiation at 40 K, t_{240} . **B**) Infrared spectrum obtained at 190 K after the warming of the sample displayed in **A**) t_{240} with a 5 K min^{-1} temperature ramp. Note: vibration mode: stretching (ν), bending (δ), rocking (ρ), torsion (τ), wagging (ω). Type of vibration mode: asymmetric (as), symmetric (s).

the corresponding photodissociation cross-section for the hydroxyacetonitrile is estimated to be $\sigma_{\text{photo}} = 8.6 \pm 1.0 \times 10^{-20} \text{ photon}^{-1} \text{ cm}^2$. In presence of water, the disappearance of $\text{HOCH}_2\text{C}^{14}\text{N}$ is thus 50% higher than the pure ice, which implies that a water environment increases the photodegradation rate of this product. The infrared monitoring of the irradiation shows that after 240 min of irradiation, the same infrared bands appear as are observed during the irradiation of the pure solid (Fig. 7A vs. Fig. 3A) with small frequency shifts due to the water environment. The bands are observed at 2340 cm^{-1} for CO_2 , at 2276 cm^{-1} for $^{13}\text{CO}_2$, at 2236 cm^{-1} for CHOCN , at 2169 cm^{-1} for NCCN , at 2136 cm^{-1} for CO , at 2088 cm^{-1} for HCN , at 2038 cm^{-1} for $\text{HN}=\text{C}=\text{CH}_2$, and at 1715 cm^{-1} for CH_2O .

The irradiated ice was then warmed from 40 K to 300 K with a temperature ramp of 5 K min^{-1} . When the temperature is approaching 180 K, the water desorbs and drives the $\text{HOCH}_2\text{C}^{14}\text{N}$ photoproducts out of the sample holder. However, after the water desorption, some $\text{HOCH}_2\text{C}^{14}\text{N}$ remains on the sample holder (Fig. 7B). $\text{HOCH}_2\text{C}^{14}\text{N}$ is effectively more refractory than water, since its desorption temperature in our laboratory conditions is around 210 K, while that of water is 180 K. Therefore, $\text{HOCH}_2\text{C}^{14}\text{N}$ can still remain on the sample holder

after the water desorption, which implies that $\text{HOCH}_2\text{C}^{14}\text{N}$ initially diluted in a water ice can be photodegraded under UV irradiation either in water ice or as a pure solid, depending on the temperature in astrophysical environments.

4. Astrophysical implications

The detection of amino acids in various meteorites leads to a search for some chemical pathways that could explain their formation in these media. One possible pathway that is relevant for the synthesis of some of them is the Strecker synthesis (Fig. 1) (Lerner & Cooper 2005). The major hypothesis is that this reaction can occur inside asteroids or meteorites through a liquid phase reaction (Cronin et al. 1994; Burton et al. 2012). This reaction is also presented as one possible pathway for the formation of the aminoacetonitrile detected in the gas phase of hot cores. The various steps leading to the aminoacetonitrile can indeed occur at the surface or inside icy grains (Danger et al. 2011a, 2012). The subsequent warming-up of grains can lead to an aminoacetonitrile release in the gas phase, which could explain, at least partly, the detection of aminoacetonitrile in warm regions. When the Strecker reaction is performed using all the necessary reactants, i.e. formaldehyde, ammonia, formic acid, and hydrogen cyanide, concurrent reactions will occur. It was indeed shown that from an ice containing formaldehyde, ammonia, and hydrogen cyanide, the aminomethanol formation ($E_a = 4.5 \text{ kJ mol}^{-1}$, Bossa et al. 2009) competes with that of hydroxyacetonitrile ($E_a = 3.9 \text{ kJ mol}^{-1}$, Danger et al. 2012). At this time, the only available rotational spectrum of these molecules is that of aminoacetonitrile. Aminomethanol and hydroxyacetonitrile cannot be detected yet due to the lack of their respective rotational spectra. Therefore, it could be interesting to perform such an analysis for each compound.

In this contribution, considering that the aminoacetonitrile is detected in the gas phase (Belloche et al. 2008), that the aminomethanol is supposed to have band contributions in the W33A spectrum (Bossa et al. 2009), and that the hydroxyacetonitrile is formed under the same conditions as aminomethanol at the surface or inside icy grains (Danger et al. 2012), the presence of hydroxyacetonitrile in these objects is likely, and it should be available for subsequent photoreactivity. The hydroxyacetonitrile photodegradation was therefore investigated in the laboratory at 40 K through UV irradiation using an H_2 discharge lamp with a photon flux of $2 \times 10^{15} \text{ photons cm}^{-2} \text{ s}^{-1}$. Depending on the grain position with regard to the nearby star, molecules carried on these grains can be submitted to UV irradiations with flux varying from 0 to $10^8 \text{ photons cm}^{-2} \text{ s}^{-1}$ (Ciesla & Sandford 2012). After 240 min of irradiation, the UV dose is $3 \times 10^{19} \text{ photons cm}^{-2}$, which could correspond to a UV dose during the time life in a nebula disk (10^6 years) of a grain submitted to $10^6 \text{ photons cm}^{-2} \text{ s}^{-1}$. In our experimental conditions, we demonstrate that the hydroxyacetonitrile is photodegraded in three primary pathways that lead to the formation of ketenimine, formylcyanide, and formaldehyde, three molecules that have been detected in the gas phase of warm regions. These photodegradation pathways occur when hydroxyacetonitrile is diluted in a water ice (Fig. 7A) as well as when hydroxyacetonitrile is irradiated in its pure form (Fig. 3A). Furthermore, experiments performed in the presence of water showed that even after the water desorption, which drives out a large part of its photoproducts from the sample holder (Fig. 7B), hydroxyacetonitrile remains at the grain surface because it is more refractory than water. Therefore, hydroxyacetonitrile can be considered to be one of the sources of various astrophysical relevant molecules, such

as formylcyanide (Remijan et al. 2008), or ketenimine (Lovas et al. 2006). Our results support the hypothesis that the formation of a large part of complex gas phase molecules detected in warm regions is mainly formed at the grain surface, as for the hydroxyacetonitrile formation or for the formation of its photoproducts, and once these molecules are formed, they can be released into the gas phase through their photodesorption or thermal desorption (Fig. 7B). The importance of hydroxyacetonitrile for the formation of these molecular species should be estimated by modelling grain evolution (Vasyunina et al. 2012).

5. Conclusion

The Strecker synthesis is presented as one possible chemical pathway for the formation of the aminoacetonitrile $\text{NH}_2\text{CH}_2\text{CN}$ in astrophysical environments. However, this reaction competes with various side reactions. One of these side reactions concerns the hydroxyacetonitrile HOCH_2CN formation in competition with the aminomethanol $\text{NH}_2\text{CH}_2\text{OH}$. Taking into account this scenario, the hydroxyacetonitrile can thus be considered as a potential astrophysical molecule that should be searched for. We investigated the hydroxyacetonitrile stability under UV irradiations and showed that its photodegradation as a pure solid gives a photodissociation cross-section of $\sigma_{\text{photo}} = 5.7 \pm 1.0 \times 10^{-20} \text{ photon}^{-1} \text{ cm}^2$ for the ^{14}N and ^{15}N isotopologues. Its irradiation after dilution in water ice gives a photodissociation cross-section of $\sigma_{\text{photo}} = 8.6 \pm 1.0 \times 10^{-20} \text{ photon}^{-1} \text{ cm}^2$. The photodegradation of the hydroxyacetonitrile leads to the formation of several molecules detected in the gas phase of hot cores. Its primary photodegradation pathway indeed leads to the formation of ketenimine, formaldehyde, hydrogen cyanide, and formylcyanide. The secondary pathways lead to the formation of hydrogen cyanide, cyanogen, carbon monoxide, and carbon dioxide. Furthermore, since hydroxyacetonitrile is more highly refractory than water, its photodegradation can occur in water ice as well as at the surface of grains after the water desorption. During the grain cycle, grains can be warmed, which could provide the release into the gas phase of hydroxyacetonitrile photoproducts. Hydroxyacetonitrile can therefore be considered as a potential source of gas phase molecules detected in astrophysical environments.

Acknowledgements. This work was funded by the French national program Physique Chimie du Milieu Interstellaire (P.C.M.I), Environnements Planétaires et Origines de la Vie (EPOV) and the Centre National d'Études Spatiales (C.N.E.S.).

References

- Belloche, A., Menten, K. M., Comito, C., et al. 2008, *A&A*, 482, 179
 Biele, J., & Ulamec, S. 2008, *Space Sci. Rev.*, 138, 275
 Borget, F., Danger, G., Duvernay, F., et al. 2012, *A&A*, 541, A114
 Bossa, J. B., Theule, P., Duvernay, F., & Chiavassa, T. 2009, *ApJ*, 707, 1524
 Brownlee, D., Tsou, P., Anderson, J., et al. 2003, *J. Geophys. Res. Planets*, 108
 Burton, A. S., Stern, J. C., Elsila, J. E., Glavin, D. P., & Dworkin, J. P. 2012, *Chem. Soc. Rev.*, 41, 5459
 Caro, G., Meierhenrich, U., Schutte, W., et al. 2002, *Nature*, 416, 403
 Ceccarelli, C. 2008, in *IAU Symp.*, 251, 79
 Ciesla, F. J., & Sandford, S. A. 2012, *Science*, 336, 452
 Cottin, H., Moore, M., & Benilan, Y. 2003, *ApJ*, 590, 874
 Cronin, J., Cooper, G., & Pizzarello, S. 1994, *Adv. Space Res.*, 15, 91
 Danger, G., Borget, F., Chomat, M., et al. 2011a, *A&A*, 535, A47
 Danger, G., Bossa, J. B., de Marcellus, P., et al. 2011b, *A&A*, 525, A30
 Danger, G., Duvernay, F., Theulé, P., Borget, F., & Chiavassa, T. 2012, *ApJ*, 756, 11
 Dartois, E. 2005, *Space Sci. Rev.*, 119, 293
 de Marcellus, P., Meinert, C., Nuevo, M., et al. 2011, *ApJ*, 727
 d'Hendecourt, L., & Allamandola, L. J. 1986, *A&AS*, 64, 453
 Duvernay, F., Chiavassa, T., Borget, F., & Aycard, J. 2004, *Chem. Phys.*, 298, 241
 Duvernay, F., Chatron-Michaud, P., Borget, F., Birney, D. M., & Chiavassa, T. 2007, *Phys. Chem. Chem. Phys.*, 9, 1099
 Elsila, J. E., Glavin, D. P., & Dworkin, J. P. 2009, *Meteor. Planet. Sci.*, 44, 1323
 Fayolle, E. C., Bertin, M., Romanzin, C., et al. 2011, *ApJ*, 739, L36
 Fraser, H., McCoustra, M., & Williams, D. 2002, *Astron. Geophys.*, 43, 10
 Frisch, M., Trucks, G., Schlegel, H., et al. 1998, *Gaussian 98*, revision A8, 25
 Garrod, R. T., Weaver, S. L. W., & Herbst, E. 2008, *ApJ*, 682, 283
 Gaudry, R. 1955, *Organic Syntheses Coll.*, 3, 436
 Gerakines, P., Schutte, W., Greenberg, J., & Vandishoeck, E. 1995, *A&A*, 296, 810
 Greenberg, L. T. 1973, 52, 413
 Gulkis, S., & Alexander, C. 2008, *Space Sci. Rev.*, 138, 259
 Herbst, E., & van Dishoeck, E. F. 2009, *ARA&A*, 47, 427
 Hudson, R., & Moore, M. 2004, *Icarus*, 172, 466
 Jacox, M., & Milligan, D. E. 1963, *J. Am. Chem. Soc.*, 85, 278
 Lee, C., Yang, W., & Parr, R. 1988, *Phys. Rev.*, 37, 785
 Lerner, N., & Cooper, G. 2005, *Geochim. Cosmochim. Acta*, 69, 2901
 Lewis-Bevan, W., Gaston, R., Tyrrell, J., Stork, W., & Salmon, G. 1992, *J. Am. Chem. Soc.*, 114, 1933
 Lovas, F. J., Hollis, J. M., Remijan, A. J., & Jewell, P. R. 2006, *ApJ*, 645, 137
 Noble, J., Congiu, E., Dulieu, F., & Fraser, H. J. 2012a, *MNRAS*, 421, 768
 Noble, J., Theule, P., Borget, F., et al. 2012b, *MNRAS*, accepted
 Remijan, A., Sutton, E., Snyder, L., et al. 2004, *ApJ*, 606, 917
 Remijan, A. J., Hollis, J. M., Lovas, F. J., et al. 2008, *ApJ*, 675, 85
 Schutte, W., Allamandola, L., & Sandford, S. 1993, *Icarus*, 104, 118
 Stroh, F., Winnewisser, B., Winnewisser, M., et al. 1989, *Chem. Phys. Lett.*, 160, 105
 Throop, H. B. 2011, *Icarus*, 212, 885
 Vasyunina, T., Vasyunin, A. I., Herbst, E., & Linz, H. 2012, *ApJ*, 751, 105
 Watanabe, N., & Kouchi, A. 2008, *Prog. Surf. Sci.*, 83, 439